TROPICAL CYCLONE LANDFALL UNDER THE INFLUENCE OF UNIFORM FLOW

WILLIAM C. T. SHUM AND JOHNNY C. L. CHAN*
Laboratory for Atmospheric Research
Department of Physics and Materials Science, City University of Hong Kong

1. INTRODUCTION

The landfall problem of tropical cyclones (TCs) has attracted much scientific attention in recent years since it was highlighted in the U.S. Weather Research Program (Marks et al. 1998). Widespread destruction of life, property and infrastructure occurs when a tropical cyclone makes landfall over a densely populated region. Therefore, the structural evolution of a TC near landfall is also of important social and economic interest. Both observational and numerical simulations of landfalling TCs have revealed that asymmetric structures can develop from symmetric vortices during the landfall process. Powell (1987) emphasized the existence of a land-sea frictional asymmetry for Hurricane Alicia in 1983, with frictional convergence more pronounced to the right of the storm. Hurricane Danny in 1997 (Blackwell 2000) underwent a rapid asymmetric transition from an original highly symmetric structure before landfall, with intense convection and maximum rainfall developing in the western eyewall. Three out of the four landfalling TCs in Hong Kong in 1999 also exhibited enhanced convection in the mid- to lower troposphere in the frontal-left quadrant of the TC center ranging from 6-18 h before landfall (Chan et al. 2004). As pointed out by Powell (1982), such development of asymmetries may result from the combined effects of land-sea roughness differences, basic environmental steering flow and translational motion of the storm.

Numerical experiments have been performed by Tuleya et al. (1984, referred as TBK84), and Chan and Liang (2003, referred as CL03) to understand the physical processes associated with TC landfall. However, in both studies, the landfall process was simulated by moving the coastline towards the vortex. A more realistic scenario is to move the vortex towards the coastline with a uniform flow. As pointed out by Kwok and Chan (2005, referred as KC05), vortex tilt and midlevel warming can develop in TCs under persistent influence of uniform flow, with tilted and deformed potential vorticity at the upper levels. These effects are omitted in TBK84 and CL03.

The objective of this study is therefore to investigate the changes in the structure of a tropical cyclone (TC) during landfall under easterly flows of uniform strength 4, 6 or 8 m s^{-1} on an *f* plane. Idealized numerical experiments are performed using the fifth-generation Pennsylvania State University – National Center for Atmospheric Research Mesoscale Model (MM5) version 3.7. In section 2, the model configurations and the experimental design are described. The results, including the intensity changes and the asymmetric structure of the TCs, are presented in section 3. A brief summary and some concluding comments are included in section 4.

* *Corresponding author address:* Johnny C.L. Chan, Department of Physics and Materials Science, City University of Hong Kong, Tat Chee Ave., Kowloon, Hong Kong, China
Email:Johnny.Chan@cityu.edu.hk

2. MODEL CONFIGURATION AND EXPERIMENTAL DESIGN

A single 8-km resolution domain, with both 511 grid points in the meridional and zonal directions, is used in all MM5 simulations of this study. The domain covers an area of 4088 km × 4088 km. There are 23 vertical model layers with the top level at 50 hPa. All the experiments are performed on an *f* plane with the Coriolis parameter fixed at 15°N.

The numerical experiments are divided into two groups: the control group and the landfall group (Table 1). For the control group experiments, all grid points in the entire domain are set to be water bodies. For the landfall group experiments, 511×170 grid points in the westernmost part of the domain are set to be 'land', while the remaining grid points are set to be water bodies. The coastline is therefore oriented in a north-south direction. The roughness length (z_o) of land is 50 cm in the landfall group experiments, while the roughness length of water bodies is 0.01 cm in all experiments. The moisture availability of both land and water bodies is set at 100%. The surface temperature over land and sea is fixed at 28.5°C in all experiments. Other properties of land and water bodies are defaulted according to Category 1 and Category 16 of the MM5 model specification.

The simple ice moisture scheme (Dudhia 1989) and the Eta planetary boundary layer scheme (Janjić 1990, 1994) are chosen to model the moisture and the boundary layer physics respectively. Atmospheric radiation is switched off in all experiments. No cumulus scheme is used since the domain resolution is fine enough.

In all simulations, a bogus vortex is first spun up in a quiescent atmospheric environment for 30 h with the inclusion of the above physical processes. The initial vortex has a minimum sea level pressure (MSLP) of 975 hPa and a radius of 15 m s^{-1} winds of 400 km. The spun-up vortex has a MSLP of 955 hPa. Easterly flows of 4, 6, 8 m s^{-1} are superimposed on the spun-up vortex to create the initial conditions in all experiments (Table 1). The imposed wind fields are zonally uniform at all sigma (σ) levels. The initial positions of the spun-up bogus vortex are different among experiments of different uniform flow strength, so that the storm spends roughly the same time (about 50 - 55h) over the water bodies in the landfall group experiments. It is obvious that the bogus vortices in experiments CU[8] and LU[8] have to be

placed farther away from the coastline than the vortices in experiments CU[4] and LU[4], because of the faster moving speed of the former two vortices.

Uniform flow speed (m s^{-1})	Control group experiment	Landfall group experiment
4	CU[4]	LU[4]
6	CU[6]	LU[6]
8	CU[8]	LU[8]

Table 1 The list of experiments with easterly flows of different speeds

3. RESULTS

3.1 *Intensity changes of vortices*

The temporal variations of the intensities of the vortices in all experiments are shown in Fig. 1. Over most of the simulation time, the vortex in CU[4] is the strongest within the control group experiments. It gradually intensifies from 955 hPa to a maximum intensity of 903 hPa at t = 64 h. The vortex in CU[6] has its intensity changes very similar to that of the vortex in CU[8], both reaching a maximum intensity of around 910 hPa near the end of the simulation time. Such a result is fairly consistent with KC05, indicating that a stronger uniform flow suppresses TC intensification.

For the landfall group experiments, the vortices have their intensity variation similar to their respective control group experiments before landfall (t = 52 h for all LU experiments). After landfall, the TC under the strongest uniform flow weakens the fastest. The vortex in LU[8] weakens to an intensity of 951 hPa at t = 72 h from 916 hPa at landfall, an increase of 35 hPa in 20 h. During the same period, the vortices in LU[4] and LU[6] only weaken by about 25 – 29 hPa while moving over land. It appears that a stronger uniform flow may also result in faster weakening of the TC after landfall, apart from suppressing intensification over open water.

3.2 *Total wind distribution asymmetries*

The total wind distribution at σ=0.995 is firstly discussed in all experiments. A jet is found almost exactly in the right quadrant of the storm at t = 30 h (not shown). This is easily understood as the superposition of the easterly flow and the cyclonic circulation of the vortices.

However, the pattern of total wind asymmetries changes substantially as the storm moves nearer to the coastline in the landfall group experiments. The total wind distribution at σ=0.995 shows a jet with a maximum of ~55 m s^{-1} in the offshore quadrant of the storm, just prior to landfall (t = 51 h for all LU experiments, LU[8] case shown in Fig. 2). At the instant when the storm makes landfall (t = 52 h), an abrupt decrease in wind speed (LU[8] case shown in Fig. 3a) occurs in the onshore quadrant because of the immediate effect of land roughness. This is consistent with the results of the maximum low-level wind distribution obtained by TBK84.

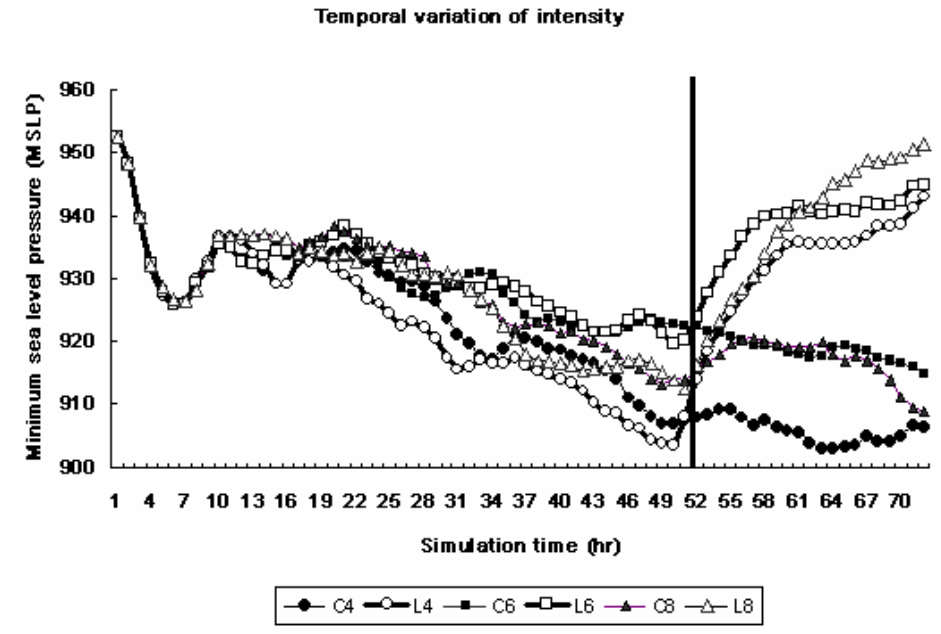

Fig. 1 Intensity evolution of vortices in all experiments (MSLP unit: hPa). The dark solid line indicates the landfall time for the LU cases.

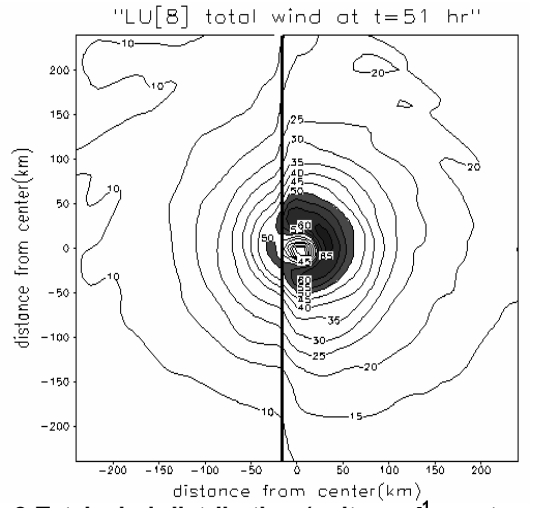

Fig. 2 Total wind distribution (unit: m s^{-1}, contour interval: 5) at sigma = 0.995 at t = 51 h for the LU[8] case. Shaded region indicates wind speeds larger than 50 m s^{-1}. Dark vertical line indicates the coastline.

(a)

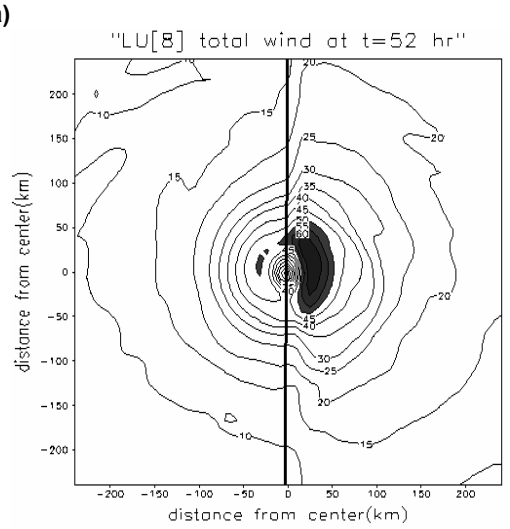

(b)

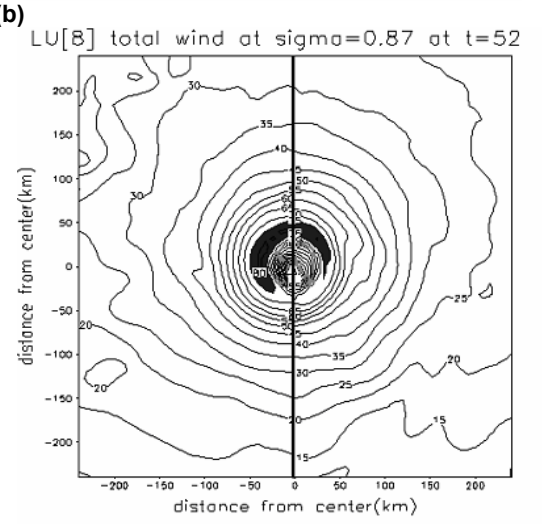

Fig. 3 Total wind distribution (unit: m s^{-1}, contour interval: 5) at t = 52 h of LU[8] case at sigma level of (a) 0.995 (b) 0.87. Shaded region indicates wind speeds larger than (a) 50 m s^{-1} (b) 70 m s^{-1}. Dark vertical line indicates the coastline.

Further examination of the total wind at a slight higher level of σ = 0.87 shows, however, another asymmetric pattern. The jet of maximum wind (~ 70 m s^{-1}) is located in the frontal-right quadrant in all LU cases (LU[8] case shown in Fig. 3b). This indicates that a region of high vertical wind shear exists in the onshore quadrant, which is consistent with the observations in Hurricane Alicia at landfall (Powell 1987).

As the storm moves further inland (t = 54 h), the region of maximum wind at σ = 0.995 tends to stay off the coastline, lagging behind the surface center of the storm (LU[8] shown in Fig. 4). Such result is also found in TBK 84.

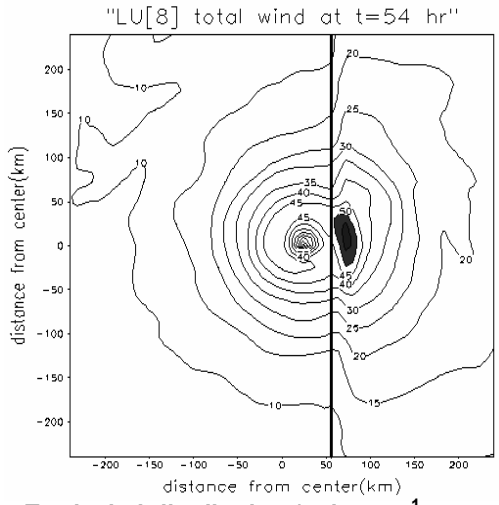

Fig. 4 Total wind distribution (unit: m s^{-1}, contour interval: 5) at sigma = 0.995 at t = 54 h for LU[8] case. Shaded region indicates wind speeds larger than 50 m s^{-1}. Dark vertical line indicates the coastline.

3.3 *Vertical wind shear (VWS)*

Two sets of VWS are computed for all the experiments: the first set (σ-level VWS) between the upper σ = 0.87 and lower σ = 0.995 levels, and the second set (pressure level VWS) between the upper (200 hPa) and lower (850 hPa) levels. The computation is similar to that of Wong and Chan (2004, hereafter WC04) and KC05: the zonal and meridional winds at σ = 0.87 (200hPa) and σ = 0.995 (850 hPa) are interpolated onto an 8 km x 5^{o} azimuth polar grid relative to the vortex center. Area averaging of the shear is then performed on a 400-km disc, which is the region with the most temporal variations of the shear (WC04).

The σ-level VWS is quite stable in the control group experiments. Southeasterly shear is observed in all CU cases (Fig. 5), with only little temporal variation in their magnitude. For the landfall group experiments, however, the σ-level VWS tends to change from southeasterly to east or east-northeasterly as the TC moves from open water to land (Fig. 5). The magnitude of such VWS also increases soon after landfall, with the maximum VWS occurring in the case of LU[8] (Fig. 6). As mentioned in section 3.2, the pattern of total wind distribution asymmetries is very different between the σ = 0.995 and σ = 0.87 levels

during landfall. The abrupt decrease in wind speed in the onshore quadrant at σ = 0.995 at landfall is likely to contribute to the changes in the direction of σ-level VWS and its increase in magnitude as the storm crosses the coastline.

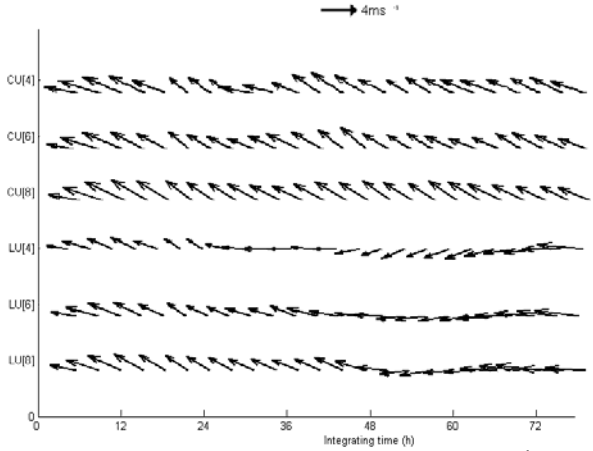

Fig. 5 Time evolution (3 h interval, unit : m s^{-1}) of σ-level (σ = 0.87 – 0.995) VWS vectors for all cases.

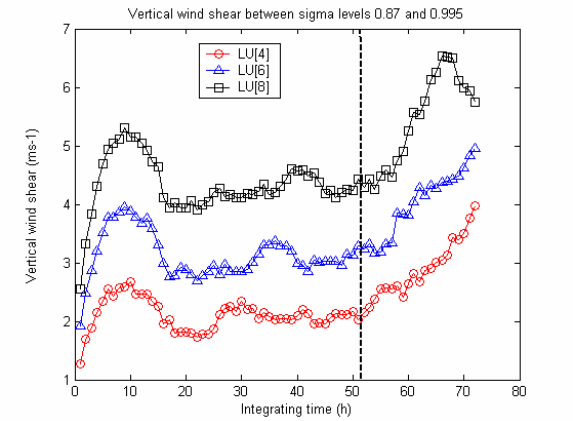

Fig. 6 Temporal variations of the 0-400 km area-averaged total σ-level shear (σ = 0.87 – 0.995, unit: m s^{-1}) for cases LU[4], LU[6] and LU[8]. The dark dashed line denotes the landfall time.

Compared with the σ-level VWS, the pressure level VWS, however, shows obviously more fluctuations in all experiments (Fig. 7). For the control group experiments, such shear is generally northeasterly in the first half of the simulation time. Towards the end of the simulation, it changes to southwesterly in the case of CU[4], but southeasterly in the cases of CU[6] and CU[8]. For the landfall group experiments, the temporal variation of the pressure level VWS is similar to their respective control experiment in the first half of simulation time. In the cases of LU[4] and LU[8], the magnitude of such shear is much larger than that of CU[4] and CU[8] respectively after landfall. The direction of the shear vector, however, does not show significant differences with the respective control cases. At the instant when the storm makes landfall, west-northwesterly shear is observed in the cases of LU[4] and LU[6], while east-southeasterly shear is observed in the case of LU[8].

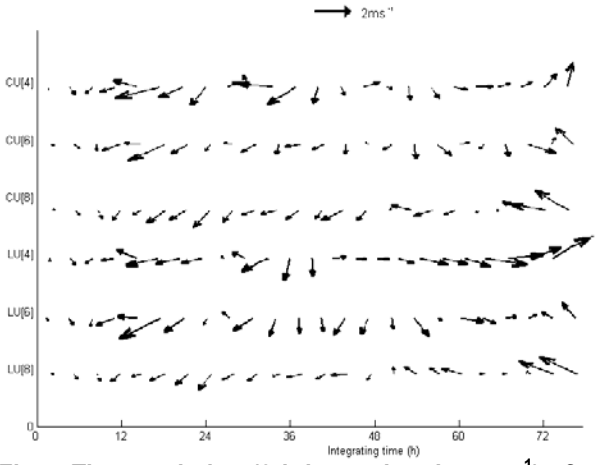

Fig. 7 Time evolution (3 h interval, unit : m s^{-1}) of pressure level (200 – 850 hPa) VWS vectors for all cases

3.4 *Vertical motion and rainfall asymmetries*

The vertical motion distribution at both levels σ = 0.91 and σ = 0.525 are investigated in all cases. Temporal variation of vertical motion distribution at each of these two σ levels is obtained similar to the computation of VWS in section 3.3: the vertical velocities at σ = 0.91 and σ = 0.525 are interpolated separately onto a 8 km x 1° azimuth polar grid relative to the vortex center. Area averaging is then performed on a 104-km disc at each azimuth direction, within which most of the vertical motion variation is found.

Stronger rising motion at σ = 0.91 is found in the northwest quadrant of the vortices in all experiments (LU[8] case shown in Fig. 8) throughout the simulation period, but more obvious in the landfall group cases. As the storm moves from open sea to inland, the rising motion at σ = 0.91 in the northwest quadrant is further enhanced in all LU cases (LU[8] case shown in Fig. 9) till the end of simulation time.

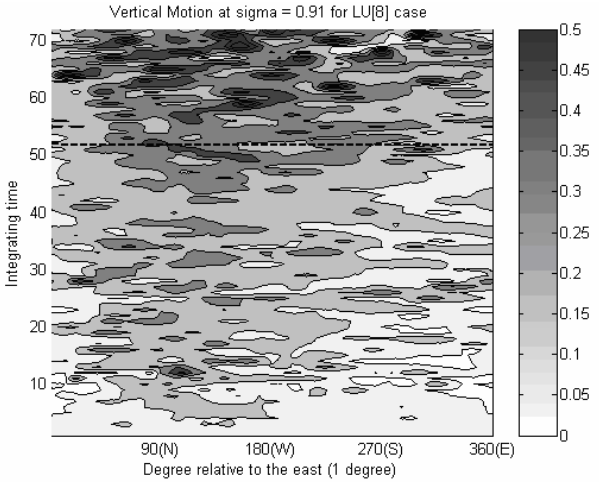

Fig. 8 Temporal variation of the vertical motion at sigma = 0.91 (unit: m s^{-1}, contour: 0.1) averaged within 104 km from the TC surface center at each azimuth for experiment LU[8]. Shading indicates rising motion. The dashed line indicated the time of landfall.

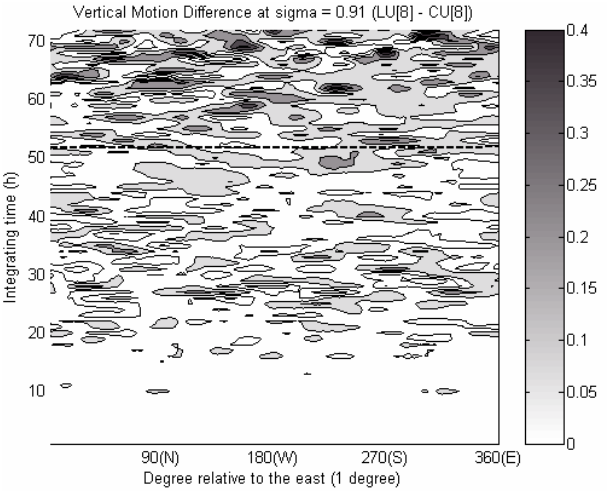

Fig. 9 Temporal variation of vertical motion difference at sigma = 0.91 (unit: m s^{-1}, contour: 0.06) averaged within 104 km from the TC surface center at each azimuth for LU[8] case relative to that of CU[8] case. Shading indicates positive values. The dashed line indicated the time of landfall for the LU[8] case.

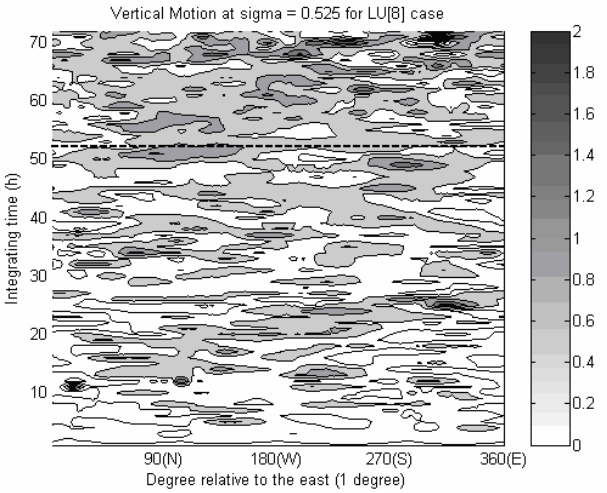

Fig. 10 Temporal variation of the vertical motion at sigma = 0.525 (unit: m s^{-1}, contour: 0.3) averaged within 104 km from the TC surface center at each azimuth for experiment LU[8]. Shading indicates rising motion. The dashed line indicated the time of landfall.

As mentioned by WC04, considerable vertical motion asymmetries could develop even under very small VWS. The asymmetric vertical motion at σ = 0.91 is likely to be developed as a result of the southeasterly or easterly σ-level VWS (see Fig. 5). As the magnitude of σ-level VWS increases after landfall in the landfall group experiments, the vertical motion at σ = 0.91 becomes more asymmetric after landfall.

The vertical motion distribution at σ = 0.525 in all cases also shows asymmetric patterns (LU[8] case shown in Fig. 10), but less obvious as compared with the distribution at σ = 0.91. The region of rising motion at σ = 0.525 tends to rotate cyclonically. Just prior to landfall, stronger rising motion at σ = 0.525 is found in the northwest quadrant in the LU[4] case (not shown), but in both the northwest and south quadrants in the LU[6] (not shown) and LU[8] (Fig. 10) cases. The rising motion at σ = 0.525 shows enhancement in some of the quadrants after landfall (LU[8] case shown in Fig. 11).

Temporal variation of hourly rainfall is obtained using the same interpolation and averaging method as in the case of vertical motion distribution. The radius of 104 km is also chosen. For the LU[6] and LU[8] cases (LU[8] case shown in Fig. 12), maximum rainfall is found in the south to southwest quadrant of the storm just before landfall. Such asymmetric rainfall pattern is less obvious in the LU[4] case (not shown). This result is fairly consistent with that in CL03. Such region of maximum rainfall in the LU[6] and LU[8] cases appears to be downstream of the strong rising motion at σ = 0.91. It agrees with the orientation of σ level VWS but does not agree with the orientation of pressure level VWS for the LU[6] case.

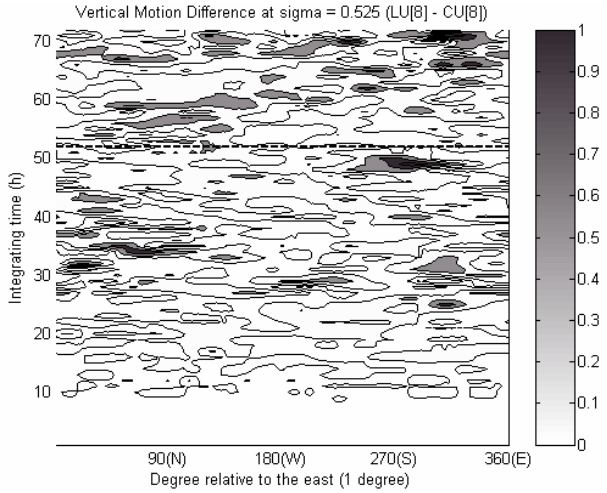

Fig. 11 Temporal variation of the vertical motion difference at sigma = 0.525 (unit: m s^{-1}, contour: 0.2) averaged within 104 km from the TC surface center at each azimuth for LU[8] case relative to that of CU[8] case. Shading indicates positive values. The dashed line indicated the time of landfall of LU[8].

The increase in rainfall of the landfall group experiments as compared with the respective control cases is also computed (LU[8] case shown in Fig.13). It is found that more rainfall is produced in almost all quadrants of the TC soon after landfall, which may be related to the enhanced rising motion at σ = 0.91 over land. However, no significant increase in rainfall in particular quadrants is found in the landfall group experiments when compared with their respective controls. This may reveal that it is the influence of uniform flow playing the major role in dominating the location of maximum landfall in our experiments.

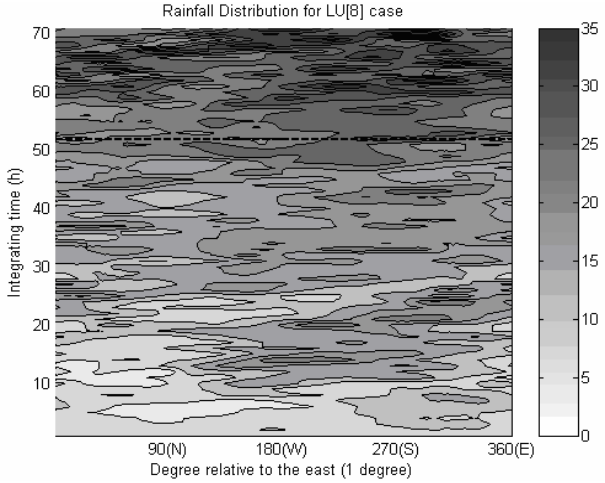

Fig. 12 Temporal variation of the hourly rainfall (unit: mm, contour: 5) averaged within 104 km from the TC surface center at each azimuth for experiment LU[8]. The dashed line indicated the time of landfall.

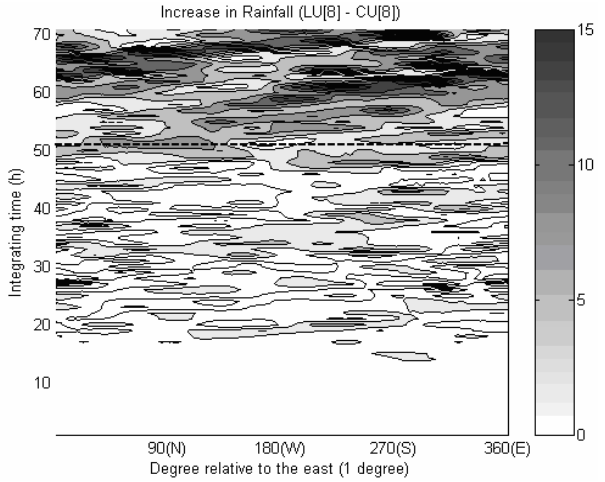

Fig. 13 Changes in hourly rainfall (unit: mm, contour: 3) averaged within 104 km from the TC surface center at each azimuth for LU[8] case relative to that of CU[8] case. Shading indicates increase in rainfall. The dashed line indicated the time of landfall for the experiment of LU[8].

3.5 *Vortex tilt and temperature anomaly*

As pointed out by WC04, one of the major mechanisms for TC weakening under high VWS is the existence of vortex tilt. The zonal and meridional cross section of the potential vorticity (PV) patterns is studied in the landfall group experiments to look for possible existence of vortex tilt, especially near the instant of landfall. It is found that PV tilting is not obvious at mid- to upper levels (levels above 700 hPa), but some tilting is noticeable at lower levels (levels below 700 hPa). At t = 52 h, the low-level PV is slightly tilted to the east in LU[4] case (not shown), and slightly to the southeast in LU[6] (not shown) and LU[8] cases (not shown).

As pointed out by DeMaria (1996), the tilted PV can be associated with an increased mid-level warming near the TC center, suppressing the TC development. To perform the analysis, temperatures at each σ level are interpolated onto a 8 km x 5^{o} azimuth polar grid relative to the vortex center. The temperature anomaly is the temperature within a 80-km averaged vortex core in the landfall cases relative to that of the control cases.

As shown in Fig. 14, midlevel warming begins just prior to landfall and persists till the end of simulation in experiment LU[8]. An increased temperature anomaly of about 0.5 – 1K is observed between the levels σ=0.525 and σ=0.775 in LU[8] case relative to CU[8] case. On the other hand, a decreased temperature anomaly of about 2 – 2.5 K is observed in the upper levels. Similar midlevel warming and upper-level cooling is also observed in LU[4] and LU[6] cases (not shown). Such results are similar to that of KC05 who computed the temperature anomaly of the uniform flow cases relative to the no-flow case. The degree of midlevel warming and upper level cooling is, however, less obvious when compared with that in KC05. This is reasonable as the tilting in PV is more observable in the cases of KC05. The existence of such midlevel warming, even of a smaller extent in our cases, may still one of mechanisms contributing to TC weakening after landfall.

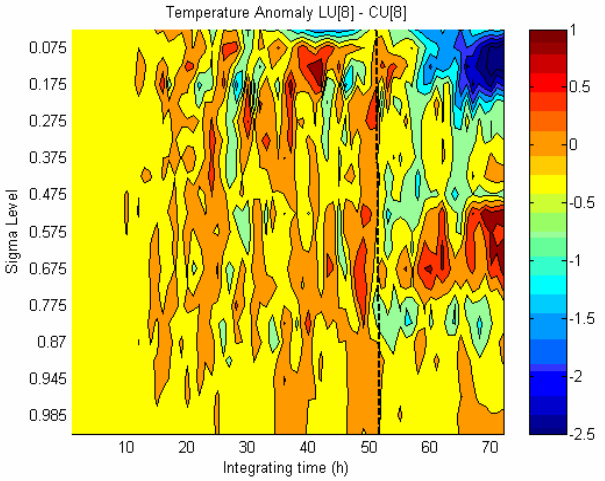

Fig. 14 Temporal variation of temperature anomalies (unit: K, contour: 0.5) at each σ level for LU[8] case relative to that of CU[8] case. The dashed line indicates the time of landfall in the LU[8] case.

5. *Summary and concluding remarks*

This paper presents structural evolution of TCs making landfall under the steering of a uniform flow. Asymmetries in total wind distribution, vertical motion, rainfall and PV are observed in all the landfall group cases. Some of these asymmetric structures are likely to contribute the weakening of the TC after landfall.

During landfall, the location of low-level maximum wind at σ = 0.995 is found in the offshore quadrant while at σ = 0.87 is found in the onshore quadrant in all landfall group experiments. A region of high vertical

wind shear exists in the onshore side. Actual calculation of VWS between these 2 σ levels shows an increase in magnitude after landfall, with the maximum σ-level VWS occurring in the LU[8] case. This is also the case where the vortex weakens the fastest over land. Relatively steady east or southeasterly σ-level VWS is found in all cases. The vertical motion distribution at σ = 0.91 also shows a persistent asymmetric pattern with the strongest rising motion in the northwest quadrant in most cases. For the LU[6] and LU[8] cases, the region of maximum hourly rainfall is likely to be downstream of the strong rising motion at σ = 0.91.

The pressure level VWS, however, demonstrates a less stable pattern. Its magnitude is generally smaller to that of the σ-level VWS. The vertical motion distribution at σ = 0.525 also shows a less asymmetric pattern when compared with that at σ = 0.91. The region of maximum rising motion at σ = 0.525 tends to rotate cyclonically.

Maximum rainfall is observed in south to southwest quadrant of the vortex just before landfall in LU[6] and LU[8] cases. However, no significant increase in rainfall in particular quadrants is found in the landfall group experiments when compared with their respective controls. This may reveal that it is the influence of uniform flow playing the major role in dominating the location of maximum landfall in our experiments.

Tilting in mid- to upper level PV is not obvious in the landfall group experiments, but slight tilting in low level PV can be observed. A midlevel warming is found such that the vortices in the landfall cases have an increased temperature anomaly in the midlevels relative to their respective control runs.

To summarize, in addition to frictional dissipation, the strong σ-level VWS and the subsequent midlevel warming developed during and after landfall may be one of the mechanisms contributing to the weakening of TC over land. It should be noted that, however, the strong uniform flow can be the dominant factor in some of the observed asymmetries, even though the inclusion of such background steering flow gives a more realistic atmospheric picture.

Acknowledgements. This research is sponsored by the Research Grant Council of the Hong Kong Special Administrative Region, China Grant CityU 100203

References:

Blackwell, G. K., 2000: The evolution of Hurricane Danny (1997) at landfall: Doppler-observed eyewall replacement, vortex contraction/intensification, and low-level wind maxima., *Mon. Wea Rev.,* **128,** 4002-4016

Chan, J. C. L. and X. Liang, 2003: Convective Asymmetries associated with tropical cyclone landfall. Part I: f-plane simulations. *J. Atmos. Sci*., **60**, 366-376

—, K. S. Liu, S. E. Ching and E. S. T. Lai, 2004: Asymmetric distribution of convection associated with tropical cyclones making landfall along the South China coast. *Mon. Wea. Rev.*, **132**, 2410-2420

DeMaria, M., 1996: The effect of vertical shear on tropical cyclone intensity change, *J. Atmos. Sci.,***53,** 2076-2087

Dudhia,J.,1989: Numerical study of convection observed during the winter monsoon experiment using a mesoscale two-dimensional model., *J.Atmos. Sci.,* **46,** 3077-3107

Janjić, Z.I., 1990: Step-mountain coordinate, physical package. *Mon. Wea. Rev.,* **118**, 1249-1443.

—,1994: Step-mountain Eta coordinate model: Further developments of the convection, viscous sublayer, and turbulence closure schemes. *Mon. Wea. Rev.,* **122**, 927-945.

Kwok, J. H. Y., and J. C. L. Chan, 2005: The influence of uniform flow on tropical cyclone intensity change. *J. Atmos. Sci.,* **62,** 3193-3212.

Marks, F.D., and L.K.Shay, 1998: Landfalling tropical cyclones: Forecasting problems and associated research opportunities. *Bull. Amer. Meteor. Soc*., **79**, 305-323

Powell, M.D., 1982: The transition of the Hurricane Frederic boundary-layer wind field from the open Gulf of Mexico to landfall. *Mon. Wea. Rev.,* **110,** 1912-1932

—,1987: Changes in the low-level kinematics and thermodynamic structure of Hurricane Alicia (1983) at landfall. *Mon. Wea. Rev.*, **115**, 75-79

Tuleya, R.E., and Y. Kurihara, M.A. Bender, and Y. Kurihara, 1984: A simulation study of the landfall of tropical cyclones using a movable nested-mesh model. *Mon. Wea. Rev.*, **112**, 124-136

Wong, M. L. M., and J. C. L. Chan, 2004: Tropical cyclone intensity in vertical wind shear. *J. Atmos. Sci.,* **61,** 1859-1876.